

Classical orbit bifurcation and quantum interference in mesoscopic magnetoconductance

J. Blaschke and M. Brack

Institut für Theoretische Physik, Universität Regensburg, D-93040 Regensburg, Germany

(May 19, 2019)

We study the magnetoconductance of electrons through a mesoscopic channel with antidots. Through quantum interference effects, the conductance maxima as functions of the magnetic field strength and the antidot radius (regulated by the applied gate voltage) exhibit characteristic dislocations that have been observed experimentally. Using the semiclassical periodic orbit theory, we relate these dislocations directly to bifurcations of the leading classes of periodic orbits.

03.65.Sq, 73.20.Dx, 73.23.Ps

Since it has become feasible to laterally confine a two-dimensional electron gas (2DEG) on length scales that are considerably smaller than the mean-free path of the electrons, the connection between classical and quantum mechanics has gained an increasing renewed interest. Therefore, many experimental and theoretical investigations have recently been focused on the onset of quantum interference effects in mesoscopic ballistic devices. A well-adapted theoretical tool for this regime is the semiclassical approach that approximates quantum mechanics to leading orders in \hbar , which is conceptually quite remarkable because it links quantum interference effects to purely classical phase-space dynamics. The so-called trace formula, originally developed by Gutzwiller [1] for the density of states of a system with only isolated orbits in phase space, has been extended to systems with continuous symmetries [2,3] (see Ref. [4] for further literature) and for other physical properties such as conductance [5,6] or magnetic susceptibility [7,8]. Many quantum interference effects observed in mesoscopic systems could successfully be explained by the interference of a few classical periodic orbits, such as the Shubnikov-de Haas oscillations of the free 2DEG [5,6], the magnetoconductance oscillations of a 2DEG in an antidot superlattice [5,6,9,10] or a large circular quantum dot [11], or the current oscillations in a resonant tunneling diode (RTD) [12]. (Examples from other physical systems, e.g. nuclei and metal clusters, are given in Ref. [4].)

Most real physical systems are neither integrable nor fully chaotic, but have mixed phase-space dynamics. Varying an external parameter (e.g., deformation, magnetic field strength, or energy), such systems typically exhibit bifurcations of periodic orbits, whereby new orbits are born or old orbits vanish. In the RTD [12], period-doubling bifurcations were shown to be responsible for a period doubling in the oscillations of the observed I-V curves. In this letter, we will show a different mechanism

through which orbit bifurcations manifest themselves in the magnetoconductance of a mesoscopic device, a narrow channel with central antidots. We will present a semiclassical interpretation of characteristic dislocations in the conductance maxima as functions of antidot diameter and magnetic field strength and relate them to bifurcations of the leading classes of periodic orbits.

For the semiclassical description of the conductance we follow the approach of Refs. [5,6]. The smooth part of the conductance G_{xx} (in the direction x of the electric current) can be described by the classical Kubo formula, whereas its oscillating part δG_{xx} is approximated in terms of periodic orbits (po):

$$\delta G_{xx} = \frac{1}{\ell^2} \frac{4e^2}{h} \sum_{po} C_{xx} \frac{R_{po}(\tau_\beta) F_{po}(\tau_s)}{|\text{Det}(\tilde{M}_{po} - \mathbf{1})|^{1/2}} \cos\left(\frac{S_{po}}{\hbar} - \mu_{po} \frac{\pi}{2}\right). \quad (1)$$

Here T_{po} is the (primitive) time period and S_{po} the action (both evaluated at the Fermi energy E_F), μ_{po} the Maslov index and \tilde{M}_{po} the stability matrix of each periodic orbit [1]. The temperature T is included in the factor $R_{po}(\tau_\beta) = (T_{po}/\tau_\beta) / \sinh(T_{po}/\tau_\beta)$, with the scattering time $\tau_\beta = \hbar / (\pi k T) \approx 2.4 * 10^{-11} \text{s}$. Damping due to a finite mean-free path is given by $F_{po}(\tau_s) = e^{-T_{po}/(2\tau_s)}$, where $\tau_s = m^* \mu / e \approx 3.8 * 10^{-11} \text{s}$ is the scattering time extracted from the experimental mobility μ . $\ell \simeq 1 \mu\text{m}$ is the characteristic length of the active region, and C_{xx} is the velocity-velocity correlation function of the periodic orbit, defined by

$$C_{xx} = \int_0^\infty dt e^{-t/\tau_s} \int_0^{T_{po}} d\tau v_x(\tau) v_x(t + \tau). \quad (2)$$

Eq. (1), as well as the standard trace formula for the level density, breaks down at bifurcation points where $\text{Det}(\tilde{M}_{po} - \mathbf{1}) = 0$. This is due to the stationary phase approximation used in its derivation [1], whereby the action S is expanded up to second order around the stationary points corresponding to the periodic orbits. Near an orbit bifurcation, where two (or more) stationary points coalesce, this approximation fails and has to be replaced by higher-order expansions of the action [13]. The requirement of both treating the bifurcations locally and retaining the asymptotic Gutzwiller limit far from bifurcations is met by uniform approximations, which were developed most systematically by Sieber and Schomerus [14]. At the bifurcation points, the contributions to the

trace formula are increased by a factor $\hbar^{-\delta}$, where δ depends on the type of the bifurcation [15]. In the extreme semiclassical limit $\hbar/S \rightarrow 0$, bifurcations therefore can dominate the quantum oscillations. In real systems \hbar/S is, however, finite so that the other prefactors in the trace formula may compensate the factor $(S/\hbar)^\delta$ to an amount that depends on the specific system.

In our present application, we have modified the uniform treatment of Ref. [14]. First, we have incorporated the discrete symmetries of the present system. Second, the uniform approach requires to include also complex periodic orbits (so-called ghost orbits) which were not available in our numerical calculations. We have therefore implemented a mixed approach which combines the uniform approximation for the real orbits with a suitably adapted local approximation of the ghost orbits. For the technical details of this procedure, we refer to a forthcoming extended publication. Note that the uniform approximation [14] is restricted to isolated bifurcations; a successful general treatment of bifurcations of higher codimension (i.e., bifurcations of bifurcations) is still lacking.

The device investigated here consists of electrostatic gates confining a high-mobility 2DEG in a GaAs/GaAlAs heterostructure (see Fig. 1). The 2DEG was 82nm beneath the surface, its electron density was $\approx 3.47 \times 10^{15} \text{m}^{-2}$, and the mobility about $100 \text{m}^2 \text{V}^{-1} \text{s}^{-1}$. Four metallic gates are used to define a long, narrow channel ($5 \mu\text{m} \times 1 \mu\text{m}$). These and two circular antidot gates are contacted individually. Details about the device are presented in [16–18] and the references cited therein. All measurements were taken at $T \approx 100 \text{mK}$ using standard low-excitation AC techniques.

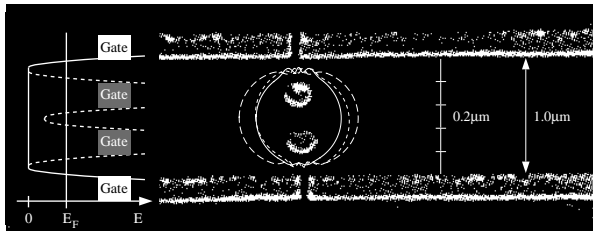


FIG. 1. SEM photograph of the gate structure [16] (without contacts). Left: Model potential used for the calculations. Center: Typical periodic orbits. Note that some of them break the discrete symmetries of the potential.

The dots in Fig. 2(a) show the experimental maximum positions of δG_{xx} as functions of magnetic field B and antidot gate voltage V_g [18]. The nearly equally spaced maxima and their shift to higher B for decreasing antidot diameter can be understood in analogy to the Aharonov-Bohm (AB) effect, if the AB ring is identified with cyclotron orbits around the antidots. Extracting the effective area from the experimental data yields a diameter between $0.76 \mu\text{m}$ and $0.86 \mu\text{m}$, which is consistent with the device dimensions. The dislocations of the

peak positions (see the boxes in Fig. 2), however, cannot be understood within this simple picture. They have been qualitatively reproduced in a quantum calculation by Kirczenov *et al.* [18].

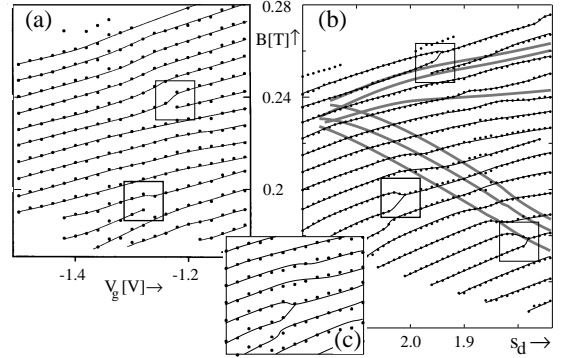


FIG. 2. Maximum positions of δG_{xx} versus magnetic field strength and gate voltage (antidot size). (a) Dots from experiment, connected with lines to guide the eye (reproduced with kind permission of the authors [18]). (b) Semiclassical results. The gray-shaded lines correspond to the loci of orbit bifurcations. (c) Behavior near a dislocation (see text), dots: experiment; lines: semiclassical results.

Our motivation for a semiclassical analysis of this system was to find out if the dislocations and the variation of the maxima spacings are genuine quantum effects (as claimed in Refs. [16,18]) or if they can be understood on a semiclassical basis. For the effective one-electron model potential we follow in spirit Kirczenov *et al.* [18] who assumed a parabolic shape $V(r) = E_F [r/a_0 - (1+s)]^2$ for $r < a_0(1+s)$ and $V(r) = 0$ otherwise. Here r denotes the distance to the gate, and a_0 gives the length scale over which the potential falls from E_F to 0, thus describing the steepness of the potential. s is a dimensionless parameter modeling the depletion width around the gates. We used $a_0 = 0.05 \mu\text{m}$ and $s = s_c = 1$ for the gates defining the channel throughout this paper. The depletion width s_d of the antidot gates was varied between 1.5 and 2.2. Following Ref. [18], this corresponds to an effective antidot diameter of $\approx 0.35 \mu\text{m}$ to $0.42 \mu\text{m}$.

As proposed by Eckhardt and Wintgen [19], we have numerically integrated simultaneously the classical equations of motion and the reduced (2D) stability matrix \tilde{M} . The orbits are converged to periodicity using the information provided by \tilde{M} . They are followed through varying B fields and antidot diameters using an adaptive extrapolation scheme. Although the potential is simple and symmetric, we find a large variety of distinct periodic orbits, many of them being asymmetric. Some typical examples are shown in Fig. 1. We included over 60 orbits (not counting their symmetry-related partners). Their actions, velocity-velocity correlation functions and periods were evaluated numerically. The Maslov index was determined using a scheme similar to that of Ref. [19].

As the orbit bifurcations are of leading order in \hbar , we now want to check if they have an increased influence on the conductance. In Fig. 3(a) we show the quantity $\text{Tr}\tilde{M}$ of three periodic orbits taking part in two successive bifurcations (where $\text{Tr}\tilde{M} = 2$) under variation of the magnetic field strength B . The left one is a tangent bifurcation, the right one a pitchfork bifurcation.

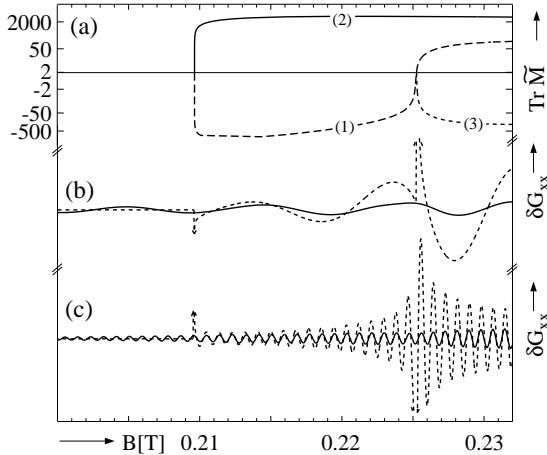


FIG. 3. (a) Trace $\text{Tr}\tilde{M}$ (note the nonlinear scale!) versus magnetic field B for three characteristic periodic orbits. (b) Contribution of all three orbits to δG_{xx} ; dotted line: Gutzwiller, solid line: uniform approximation. (c) same as (b) but for a system with 10 times larger actions.

In Fig. 3(b), the contribution of these orbits to the conductance is plotted. The dotted line gives the result of the trace formula Eq. (1). The amplitudes are diverging at the bifurcations. The uniform approximation (solid line) removes the divergences. Fig. 3(c) represents the corresponding data for a system scaled to have 10 times larger actions, thus being closer to the semiclassical limit. The amplitudes of the uniform approximation are nearly constant over the bifurcations, so that for this specific system, the lower order in \hbar does not lead to a dominant influence of the bifurcations [20].

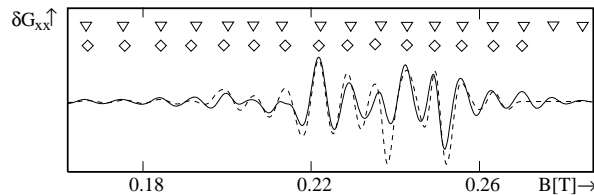


FIG. 4. δG_{xx} using the Gutzwiller (dashed line) and the uniform approximation (solid line). The maxima are marked with boxes (Gutzwiller) and triangles (uniform).

Whereas for individual orbits a uniform treatment of the bifurcations is vital, their influence becomes smaller if a larger number of orbits is included. This is demonstrated in Fig. 4, where the total δG_{xx} has been calculated for $s_d = 1.86$ including all relevant (~ 60) periodic

orbits. The solid line shows the result of the uniform approximation, whereas the dotted line corresponds to the standard Gutzwiller approach. To remove the spurious divergences in the latter case (and those due to bifurcations of higher codimension in the uniform approach), we have additionally convoluted δG_{xx} over the magnetic field B (cf. Ref. [21]). The fact that the semiclassical result depends only little on the correct treatment of the bifurcations, if many orbits are included, has already been observed in a study of the disk billiard [22]. In particular, the influence on the maximum positions (marked by boxes and triangles in Fig. 4) is small. In the following, we therefore use the trace formula Eq. (1) with additional convolution over B .

The semiclassical result for the maximum positions in δG_{xx} is shown in Fig. 2(b). We do not obtain a detailed quantitative agreement with the experimental data, since no effort has been made to optimize the model potential. Qualitatively, however, all features of the observed phase plot in Fig. 2(a) are reproduced. The spacing of the maxima will be analyzed in our extended publication, where we will also compare our results to those of quantum calculations. Presently we want to concentrate on the dislocations (see the boxes in Fig. 2), which are clearly reproduced in our semiclassical description. Fig. 2(c) shows the local behavior around the dislocations marked by the heavy boxes in (a) and (b). The points give the experimental maximum positions, and the lines correspond to the semiclassical results (with slightly shifted but unscaled values of s_d and B).

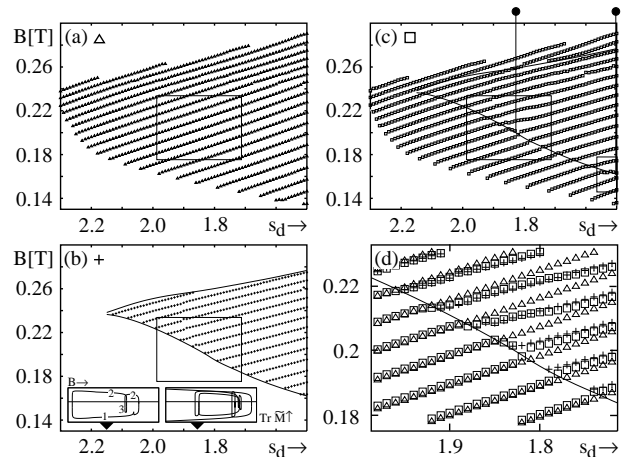


FIG. 5. Maximum positions from different orbit generations: (a) grandparents, (b) children, (c) all generations. (d) Blow-up from (a)-(c): the maxima of the total δG_{xx} (squares) follow the maxima of the children (crosses), where these exist, and those of the grandparents (triangles) otherwise.

For the semiclassical analysis of these dislocations, we consider for the moment a hypothetical system with only 7 closely related orbits. The inserts in Fig. 5(b) show $\text{Tr}\tilde{M}$ of these orbits versus B for two different antidot diameters. With decreasing s_d , new orbits are born at the bifurcations. We classify the orbits in a grandparent, a parent

and a child generation, depending if they are offsprings of orbit 1, 2, or 3, respectively. All members within a generation behave nearly identically, thus justifying our classification. The contribution of the grandparent and the child orbits to the conductance is shown in Figs. 5(a) and (b), respectively. The behavior of each generation is in complete agreement with the simple AB picture discussed above, but the effective areas and their dependence on B are different. The children have a larger semiclassical amplitude than the grandparents, thus dominating the conductance. Therefore the maxima of the total δG_{xx} closely follow the children's wishes where they exist, and the grandparents' will otherwise, as becomes clear from Fig. 5(d) (the parents' influence is negligible throughout). The different orbit generations lead to slopes and spacings of the maxima that do not match along the generation boundaries. This is the origin of the observed dislocations which occur, indeed, close to the bifurcation lines. For the real system with over 60 orbits, the effects follow the same pattern. Since there are several groups of orbits with comparable influence, the bifurcation structure seen in Fig. 2(b) (gray lines) is somewhat more complicated.

From this interpretation, we can make further predictions which have been verified numerically. (i) Scaling the system does not affect the classical dynamics, so that the dislocations must move along the (universal) bifurcation lines. (ii) Assuming a linear dependence of the action difference ΔS between children and grandparents on s_d , the dislocations are equally spaced in s_d . Scaling S with a factor κ [23], the distances between dislocations scale according to $\Delta s_d \propto \kappa$.

In summary, our semiclassical description successfully reproduces all main features observed experimentally in the magnetoconductance of a mesoscopic channel with antidots. We have analyzed especially the dislocations of the conductance maxima as functions of magnetic field B and antidot diameter s_d , and show that these are related to bifurcations of the leading classical periodic orbits of the system. The dislocations are due to the fact that the bifurcations define the border lines between regimes of different predominant orbit generations, leading to different dependences of the conductance maxima on B and s_d . This induces the observed dislocations of the maximum positions, in analogy to lattice defects at interfaces. As the classical dynamics are not affected by a rescaling of the system, the scaling behavior of the dislocations can be easily understood in the semiclassical approach.

The way in which the orbit bifurcations affect the quantum oscillations here is quite different from the one reported for the RTD [12]. There the bifurcations lead to a period doubling, whereas in the system considered here the periods of all relevant orbits are approximately constant. Furthermore, in the RTD only a few orbits were found to be important, whereas the present system is dominated by a much larger number of orbits with

nearly identical actions, periods and amplitudes. It is the subtle interplay of their slowly varying contributions under the variation of the system parameters that causes the dislocations in the phase plots of the conductance maxima. Note also that this mechanism is different from that described in connection with superdeformed nuclei [24] or an elliptic billiard [25] where period doubling orbit bifurcations influence the quantum shell structure due to their dominant order in $1/\hbar$.

It is a great pleasure to thank A. Sachruda, C. Gould and P. J. Kelly for helpful discussions and for providing us with the experimental data.

-
- [1] M. C. Gutzwiller, *J. Math. Phys.* **12**, 343 (1971).
 - [2] V. M. Strutinsky *et al.*, *Z. Phys. A* **283**, 269 (1977).
 - [3] S. C. Creagh and R. G. Littlejohn, *Phys. Rev. A* **44**, 836 (1990); *J. Phys. A* **25**, 1643 (1991).
 - [4] M. Brack and R. K. Bhaduri, *Semiclassical Physics*, *Frontiers in Physics* Vol. 96 (Addison-Wesley, Reading, 1997).
 - [5] K. Richter, *Europhys. Lett.* **29**, 7 (1995).
 - [6] G. Hackenbroich and F. von Oppen, *Z. Phys. B.* **97**, 157 (1995); *Europhys. Lett.* **29**, 151 (1995).
 - [7] K. Richter, D. Ullmo, and R. A. Jalabert, *Phys. Rep.* **276**,1 (1996).
 - [8] K. Tanaka, *Ann. Phys.* **268**, 31 (1998).
 - [9] D. Weiss *et al.*, *Phys. Rev. Lett.* **70**, 4118 (1993).
 - [10] A. Lorke *et al.*, *Phys. Rev. B* **44**, 3447 (1991).
 - [11] S. M. Reimann *et al.*, *Z. Phys. B* **101**, 377 (1996).
 - [12] D. S. Saraga *et al.*, *Phys. Rev. E* **58**, R2701 (1998) and the references cited therein.
 - [13] A. M. Ozorio de Almeida and J. H. Hannay, *J. Phys. A* **20**, 5873 (1987).
 - [14] M. Sieber, *J. Phys. A.* **29**, 4715 (1996); H. Schomerus and M. Sieber, *J. Phys. A* **30**, 4537 (1997); M. Sieber and H. Schomerus, *J. Phys. A* **31**, 165 (1998).
 - [15] The two most important cases are $\delta = 1/6$ for tangent bifurcations and $\delta = 1/4$ for period-doubling bifurcations.
 - [16] C. Gould *et al.*, *Phys. Rev. B* **51**, 11213 (1995).
 - [17] C. Gould *et al.*, *Can. J. Phys.* **74**, S207 (1996).
 - [18] G. Kirczenov *et al.*, *Phys. Rev. B* **56**, 7503 (1997).
 - [19] B. Eckhardt and D. Wintgen, *J. Phys. A.* **24**, 4335 (1991).
 - [20] That the leading-order orbits in \hbar need not dominate alone the quantum oscillations is pointed out in Ref. [4] for the equilateral triangular billiard, where the contribution of an isolated orbit (of order $\hbar^{1/2}$ relative to the leading terms) is not negligible. The same holds for the circle billiard in a magnetic field, where skipping and cyclotron orbits contribute at different orders in \hbar [21].
 - [21] J. Blaschke and M. Brack, *Phys. Rev. A* **56**, 182 (1997).
 - [22] J. Blaschke and M. Brack, *Physica E* **1**, 288 (1997).
 - [23] This corresponds to scaling the size with κ and the magnetic field with κ^{-1} .
 - [24] K. Arita, A. Sugita and K. Matsuyanagi, *Prog. Theor. Phys. (Japan)* **100**, 1223 (1998), and earlier Refs. quoted therein.
 - [25] A. G. Magner *et al.*, *Prog. Theor. Phys. (Japan)* (1999), submitted.